JOURNAL OF GUIDANCE, CONTROL, AND DYNAMICS
Vol. 16, No. 2, March-April 1993

Time-Optimal Reorientation Maneuvers for a Combat Aircraft

Spiro Bocvarov,* Frederick H. Lutze,† and Eugene M. Cliff‡
Virginia Polytechnic Institute and State University, Blacksburg, Virginia 24061

Results are presented from a study of time-optimal attitude reorientation maneuvering for an aircraft with thrust-vectoring capability. A detailed mathematical model for attitude motions of the aircraft is developed. First-order necessary conditions for optimality are applied and a family of extremal solutions obtained for two classes of reorientation maneuvers of practical interest. The thrust-vectoring power is varied parametrically, and thus an estimate of the reduction in maneuvering time due to the thrust-vectoring enhancement of the aircraft is obtained.

I. Introduction

VARIOUS analyses have shown that emerging trends in missile and radar technologies will have a profound effect on design requirements for air-superiority vehicles. It appears that, in close-in combat, vehicles with the ability to operate at extreme angles of attack will have a decided advantage.[1-4] Designing such supermaneuverable aircraft is a complex and challenging task, and future design efforts may well lead to radically new concepts. At present, however, the preferred approach is to provide a form of thrust vectoring in which propulsive power is used to generate control moments.[5,6] At high angles of attack α, especially in the post-stall region, the effectiveness of the aerodynamic control surfaces decreases rapidly with increase in α. Thus, thrust-vectoring generated (propulsive) moments must be used to maintain control of the aircraft at high α. At low α the propulsive moments can supplement the aerodynamic control surfaces and thus increase the "agility" of the aircraft. In addition, thrust vectoring can be used for control of the aircraft in case of mechanical failure or malfunction of the aerodynamic control surfaces. Several research programs that focus on utilizing thrust-vectoring control are currently under way. Among these is the F/A-18 based High Angle-of-attack Research Vehicle (HARV) program.[7]

The flight mechanics issues can be divided into two areas: 1) analysis of changes in the velocity vector and 2) analysis of changes in the body attitude. This paper presents some results obtained in a study that focused on understanding the nature of aircraft minimum-time fuselage-reorientation maneuvering. In the study, data for the HARV were used. Accordingly, the numerical results correspond to this aircraft. However, the discussion and methodology in analyzing the results presented in the next sections are quite general.

A mathematical model of the aircraft and the interacting environment (the aerodynamic forces and moments) is derived in Sec. II. The basic ideas and assumptions in the development of the mathematical model are discussed in detail. In Sec. III a class of optimal control problems of interest is formulated and a set of necessary conditions for optimality derived by using the Minimum Principle.[8-10] This set of necessary conditions is cast into a numerical multipoint boundary-value problem (MPBVP). Subsequently, a homotopy method and the related procedure for solving the MPBVPs (and thus generating families of extremals) are briefly described.[11] In Sec. IV results relating to a family of extremal solutions for two classes of reorientation maneuvers are presented. The reduction in maneuvering time, due to the thrust-vectoring enhancement of the aircraft, is discussed and supplemented by some numerical results. In addition, the influence of some thrust-vectoring design parameters on maneuvering time is shown.

II. Mathematical Model

Simplifying Assumptions

The aircraft itself and the interacting environment represent a very complex dynamical system. However, some analyses combined with prior knowledge and experience about the problem of interest suggest that certain simplifications can be made. The study pertains to maneuvers at lower values of Mach number ($M<0.4$). Rapid reorientation at higher Mach numbers seems not to be desirable because the high accelerations the aircraft experiences in this case are unacceptable for the human pilot. Some analyses by simulation and practical experience show that, if the aircraft is reoriented rapidly from steady-state straight-line flight to a specified attitude, then during the maneuver the aircraft center of mass does not deviate significantly from the line of the original direction of motion (the reorientation maneuvers are fast enough so that the linear displacements, due to the aerodynamic forces acting on the aircraft, are very small). This fact leads to a significant simplification of the mathematical model used to represent the aircraft and the interacting environment, without any significant effect on the accuracy of the model. Accordingly, the translational motion of the aircraft is neglected and only the rotational motion of the aircraft is analyzed. One can imagine the aircraft in a wind tunnel, free to rotate about the center of mass. We are interested in how the aerodynamic control surfaces and the thrust-vectoring system can be used most effectively to reorient the aircraft from one attitude to another in minimum time.

To obtain initial results for this complex optimal-control problem, it is assumed for the moment that only "conventional" aerodynamic controls will be used, each control affecting a single axis. Thus, the ailerons are used in a differential manner for roll control, the rudders for yaw control, and the horizontal tails for pitch control (as an elevator) only. The horizontal tails can also be used for roll control. However, a better understanding of their role for pitch and roll control simultaneously would require comparative studies with the conventional results. One can also use the ailerons to generate a certain amount of yawing and pitching moment, whereas the flaps or the rudders can generate some rolling moment. "Nonconventional" use of the aerodynamic control surfaces (i.e., taking advantage of cross-coupling effects) is interesting from a theoretical standpoint and may indeed have some impact on the results for time-optimal reorientation maneuvers and on some design parameters of future aircraft. However, the au-

Presented as Paper 91-2709 at the AIAA Guidance, Navigation, and Control Conference, New Orleans, LA, Aug. 12-14, 1991; received Oct. 25, 1991; revision received April 15, 1992; accepted for publication May 29, 1992.

*Research Associate, Aerospace and Ocean Engineering Department. Member AIAA.

†Professor, Aerospace and Ocean Engineering Department. Associate Fellow AIAA.

‡Reynolds Metals Professor, Aerospace and Ocean Engineering Department. Associate Fellow AIAA.

thors believe that thorough understanding should be accumulated first for time-optimal maneuvering by using the aerodynamic control surfaces in a conventional manner only.

Reference Frames

Three reference frames are considered in the derivation of the kinematical and dynamical equations of motion. These are the (inertial) horizontal reference frame, the wind reference frame, and a body-fixed reference frame. Each of them is represented by a set of unit vectors, respectively,

$$(\hat{i}^h,\hat{j}^h,\hat{k}^h), \qquad (\hat{i}^w,\hat{j}^w,\hat{k}^w), \qquad (\hat{i}^b,\hat{j}^b,\hat{k}^b) \tag{1}$$

The orientation (attitude) of the aircraft can be described in different ways, for example, by using various sets of Euler angles (ψ,θ,φ) or Euler parameters $(\beta_0,\beta_1,\beta_2,\beta_3)$.[12,13] A mathematical model using Euler parameters is appealing since the kinematical equations are free of singularities, unlike a model with Euler angles. However, the aerodynamic moments acting on the aircraft are conventionally described in terms of the aerodynamic angles α (angle of attack) and β (sideslip angle). Thus, a mathematical model directly involving α and β as state variables would require no conversion in the calculation of the aerodynamic moments or their derivatives with respect to the state variables of the model (which appear in the adjoint-variable equations).

Based on the assumption of a model with "fixed" center of mass, it is possible to devise a set of angles α, β, and μ that can describe the attitude of the aircraft uniquely, almost everywhere. Exceptions are the orientations that correspond to sideslip angles $\beta = +90$ and -90 deg, which appear as singular points in the kinematical equations. The singularities of the model at these points did not cause serious difficulties in the numerical procedures.

The angle μ is defined and can be visualized most easily in the following manner. We consider a horizontal, Earth-fixed reference frame $(\hat{i}^h,\hat{j}^h,\hat{k}^h)$ in the wind tunnel, having the x_h axis parallel to the direction of the airstream (but directed oppositely). Because of the assumption that the motion of the center of mass of the aircraft does not deviate from a straight line (which effectively means that the airstream has a constant direction in the wind tunnel), the x_w axis of the wind reference frame $(\hat{i}^w,\hat{j}^w,\hat{k}^w)$ remains parallel to the x_h axis of the horizontal reference frame. This means that the wind reference frame is constrained to roll around the x_h axis only. In other words, $\bar{\omega}^w$, the angular velocity of the wind reference frame with respect to the horizontal frame, has a nonzero component only along its x_w axis ($q_w = r_w = 0$).

At the initial time, before the beginning of a maneuver, the wind reference frame coincides with the horizontal reference frame. This situation may correspond for example, to a steady-state level flight in the vertical plane. As the aircraft starts maneuvering and $\bar{\omega}^w \neq 0$, the relative position of the wind reference frame with respect to the Earth-fixed (local horizontal) reference frame can be uniquely specified with a roll angle, denoted by μ, the angular rate being $p_w = \mathrm{d}\mu/\mathrm{d}t$. The aerodynamic angles α and β specify uniquely the orientation of the aircraft body-fixed reference frame with respect to the wind reference frame.[14]

Kinematical Relations

According to the definition of the aerodynamic angles α and β, the transformation matrix from body-fixed reference frame coordinates to wind reference frame coordinates is given by $L_{wb}(\alpha,\beta) = L_z(\beta)L_y(-\alpha)$, where L_y and L_z are the elementary transformation matrices (single rotation around the y and z axis, respectively). Thus,

$$L_{wb}(\alpha,\beta) = \begin{bmatrix} +\cos\alpha\cos\beta & \sin\beta & +\sin\alpha\cos\beta \\ -\cos\alpha\sin\beta & \cos\beta & -\sin\alpha\sin\beta \\ -\sin\alpha & 0 & \cos\alpha \end{bmatrix} \tag{2}$$

The (relative) angular velocity of the body-fixed reference frame with respect to the wind reference frame[14] is given by

$$\bar{\omega}^{\mathrm{rel}} = \bar{\omega}^b - \bar{\omega}^w = -\hat{k}^w \frac{\mathrm{d}\beta}{\mathrm{d}t} + \hat{j}^b \frac{\mathrm{d}\alpha}{\mathrm{d}t} \tag{3}$$

If each of the vectors in Eq. (3) is represented in the wind-axes system, it follows that

$$L_{wb}\begin{bmatrix} p \\ q \\ r \end{bmatrix} - \begin{bmatrix} p_w \\ q_w \\ r_w \end{bmatrix} = -\begin{bmatrix} 0 \\ 0 \\ 1 \end{bmatrix}\frac{\mathrm{d}\beta}{\mathrm{d}t} + L_{wb}\begin{bmatrix} 0 \\ 1 \\ 0 \end{bmatrix}\frac{\mathrm{d}\alpha}{\mathrm{d}t} \tag{4}$$

where $(p,q,r)^T = \bar{\omega}_b^b$: p, q, and r are the components of the aircraft (inertial) angular velocity $\bar{\omega}^b$, in the body-fixed reference frame (the aircraft roll, pitch, and yaw rates, respectively). Equations (2) and (4) yield the following relations:

$$\begin{aligned} p_w &= +p\cos\alpha\cos\beta + \left(q - \frac{\mathrm{d}\alpha}{\mathrm{d}t}\right)\sin\beta + r\sin\alpha\cos\beta \\ q_w &= -p\cos\alpha\sin\beta + \left(q - \frac{\mathrm{d}\alpha}{\mathrm{d}t}\right)\cos\beta - r\sin\alpha\sin\beta \\ r_w &= -p\sin\alpha + r\cos\alpha + \frac{\mathrm{d}\beta}{\mathrm{d}t} \end{aligned} \tag{5}$$

Based on the assumption made earlier, $q_w = r_w = 0$, we finally get the following set of differential equations that govern the dynamics of the angles specifying the aircraft attitude (kinematical equations):

$$\begin{aligned} \frac{\mathrm{d}\alpha}{\mathrm{d}t} &= q - (p\cos\alpha + r\sin\alpha)\tan\beta \\ \frac{\mathrm{d}\beta}{\mathrm{d}t} &= p\sin\alpha - r\cos\alpha \\ \frac{\mathrm{d}\mu}{\mathrm{d}t} &= p_w = (p\cos\alpha + r\sin\alpha)\frac{1}{\cos\beta} \end{aligned} \tag{6}$$

Dynamical Relations

The Euler rigid-body rotational equations are given by the following set of differential equations:

$$\begin{aligned} I_x\frac{\mathrm{d}p}{\mathrm{d}t} &= (I_y - I_z)qr + u_x(\delta_x) \\ &\quad + \frac{\rho(h)V^2(M,h)}{2}SbC_l(\alpha,\beta,\delta_a^r,\delta_a^l,p,M,\ldots) \\ I_y\frac{\mathrm{d}q}{\mathrm{d}t} &= (I_z - I_x)rp + u_y(\delta_y) \\ &\quad + \frac{\rho(h)V^2(M,h)}{2}S\bar{c}C_m(\alpha,\beta,\delta_e^r,\delta_e^l,q,M,\ldots) \\ I_z\frac{\mathrm{d}r}{\mathrm{d}t} &= (I_x - I_y)pq + u_z(\delta_z) \\ &\quad + \frac{\rho(h)V^2(M,h)}{2}SbC_n(\alpha,\beta,\delta_r^r,\delta_r^l,r,M,\ldots) \end{aligned} \tag{7}$$

In Eqs. (7), u_x, u_y, and u_z denote the propulsive moments, generated by thrust vectoring; δ_x, δ_y, and δ_z are the corresponding controls. Besides the propulsive moments, the rigid-body dynamics depend on the dynamic pressure $\bar{q} = \rho V^2/2$ (which is a function of the altitude h and the Mach number M) and on the aerodynamic controls and the aerodynamic angles α and β (expressed through the aerodynamic moment coefficients C_l, C_m, and C_n). The body-fixed reference frame axes

coincide with the principal axes of inertia of the aircraft; I_x, I_y, and I_z are the aircraft principal moments of inertia. The longitudinal and lateral reference lengths are $\bar{c}$ (the mean aerodynamic chord) and b (the wing span), respectively. The reference area is S.

The Euler equations as shown are valid under the assumption that the aircraft is a rigid body. Actually, in the course of the maneuver there is mass change in amount and distribution (e.g., the aerodynamic control surfaces and the thrust-vectoring system deflect, the mass of the aircraft varies due to the fuel exhaust, there are aeroelastic effects, etc.). However, analyses show that these effects can be neglected, with no significant loss in the accuracy of the mathematical model. For example, the mass of the moving aerodynamic control surfaces is negligible compared with the mass of the aircraft, so their movement does not vary the mass distribution of the aircraft significantly. In the mathematical model the dynamics of the aerodynamic control surfaces are neglected since their response to pilot controls is very fast compared with the time to perform the reorientation maneuvers.

The current implementations of the thrust vectoring system can be plausibly modeled in the following way:

$$u_x(\delta_x) = u_x^{\max}\delta_x$$
$$u_y(\delta_y) = u_y^{\max}\delta_y \tag{8a}$$
$$u_z(\delta_z) = u_z^{\max}\delta_z$$

$$|\delta_x|^n + |\delta_y|^n + |\delta_z|^n \le 1.0 \tag{8b}$$

It was found that $n=2$ models the thrust-vectoring system accurately. It is also a nice choice for analytical reasons. This value was used most of the time in the study.

The aerodynamic forces and moments acting on the aircraft are very complex functions, each depending on the angles α and β as well as the Mach number, altitude, and deflections of all of the aerodynamic control surfaces. However, analyses of the aerodynamic data for the HARV show that many of these dependencies can be neglected for the problem considered. For example, the aircraft center of mass moves relative to the aerodynamic reference center due to fuel sloshing and exhaustion. However, the displacement is small and stays within a few inches from the aerodynamic reference center. Therefore, it can be assumed that the aircraft mass center coincides with the aerodynamic reference center. Thus the aerodynamic forces (lift, drag, and sideslip force) have no effect on the total aerodynamic moments acting on the aircraft. Furthermore, the Mach number and the dynamic pressure can be assumed to be constant throughout the maneuvers.

The assumption that the aerodynamic control surfaces will be used for conventional moment control allows for additional simplifications. It is assumed that there are three primary controls (Δ_a, δ_e, and δ_r) such that

$$\delta_a^r = -\delta_a^l = \Delta_a$$
$$\delta_e^r = +\delta_e^l = \delta_e \tag{9}$$
$$\delta_r^r = +\delta_r^l = \delta_r$$

where superscripts r and l refer to the right and left surface, respectively.

Under these circumstances and assumptions, an accurate representation of the aerodynamic moments and control surface effectiveness is obtained if the following functional dependencies are assumed:

$$C_l \equiv C_l(\alpha,\beta,p,\Delta_a) = C_l^0(\alpha,\beta) + C_l^\zeta(\alpha,p) + C_l^c(\alpha,\Delta_a)$$
$$C_m \equiv C_m(\alpha,\beta,q,\delta_e) = C_m^0(\alpha,\beta) + C_m^\zeta(\alpha,q) + C_m^c(\alpha,\delta_e) \tag{10}$$
$$C_n \equiv C_n(\alpha,\beta,r,\delta_r) = C_n^0(\alpha,\beta) + C_n^\zeta(\alpha,r) + C_n^c(\alpha,\delta_r)$$

where C_i^0, C_i^ζ, and C_i^c ($i \in \{l,m,n\}$) denote the rigid-body static (all control surfaces in neutral position), rate damping, and aerodynamic control surface contributions to the aerodynamic moment coefficients, respectively.

The error due to the simplifications made seems not to exceed the measurement error (in the data available for the HARV) for angles of attack less than 75 deg. The aerodynamic moment coefficients for the HARV were available in the form of table lookups, the data being given at a certain set of grid points within the intervals $\beta \in (-20 \text{ deg}, +20 \text{ deg})$ and $\alpha \in (-10 \text{ deg}, +90 \text{ deg})$. For optimization purposes, analytical *model functions* for the aerodynamic moment coefficients $(C_i^0, C_i^\zeta, C_i^c)$ were developed.[11] These model functions are parameter-dependent combinations (sums and products) of elementary (rational and transcendental) functions. The model functions are smooth and indeed have an infinite number of derivatives. The initial values of the parameters appearing in these shape functions were obtained by analyses and estimates, then adjusted either by visual comparison with the given data or by using least-squares fitting software. These model functions seem to fit the data available within no more than a 5% error.

After obtaining results for the maneuvers of interest, a simulation was performed to assess the movement of the center of mass of the aircraft when maneuvering in free flight. The results justify the assumption that the center of mass does not deviate significantly from the initial direction (effectively, the movement of the aircraft center of mass changes the aerodynamic angles α and β, when compared with the case of straight-line movement). The approach described, though not correct from a purely mathematical standpoint, is quite acceptable from an engineering standpoint and very common when analyzing complex problems in a step-by-step manner.

Scaled Mathematical Model

The mathematical model of the aircraft was scaled so that it was well posed for the numerical procedures used in the optimization software. This was done in the following manner. Let

$$\tau = kt \qquad \frac{p}{k} = P \qquad \frac{q}{k} = Q \qquad \frac{r}{k} = R \tag{11}$$

where k is a scaling constant. It follows that

$$\dot{\alpha} \equiv \frac{d\alpha}{d\tau} = \frac{d\alpha}{k\,dt} = Q - (P\cos\alpha + R\sin\alpha)\tan\beta \tag{12a}$$

$$\dot{\beta} \equiv \frac{d\beta}{d\tau} = \frac{d\beta}{k\,dt} = P\sin\alpha - R\cos\alpha \tag{12b}$$

$$\dot{\mu} \equiv \frac{d\mu}{d\tau} = \frac{d\mu}{k\,dt} = (P\cos\alpha + R\sin\alpha)\frac{1}{\cos\beta} \tag{12c}$$

The Euler rotational equations are transformed accordingly:

$$\dot{P} \equiv \frac{dP}{d\tau} = \frac{dp}{k^2\,dt} = J_x\frac{q}{k}\frac{r}{k} + \frac{1}{I_x}\frac{u_x^{\max}}{k^2}\delta_x + \frac{1}{I_x}\frac{B}{k^2}C_l(\cdots)$$

$$\dot{Q} = \frac{dQ}{d\tau} = \frac{dq}{k^2\,dt} = J_y\frac{r}{k}\frac{p}{k} + \frac{1}{I_y}\frac{u_y^{\max}}{k^2}\delta_y + \frac{1}{I_y}\frac{C}{k^2}C_m(\cdots) \tag{13}$$

$$\dot{R} \equiv \frac{dR}{d\tau} = \frac{dr}{k^2\,dt} = J_z\frac{p}{k}\frac{q}{k} + \frac{1}{I_z}\frac{u_z^{\max}}{k^2}\delta_z + \frac{1}{I_z}\frac{B}{k^2}C_n(\cdots)$$

where

$$J_x = \frac{I_y - I_z}{I_x} \qquad J_y = \frac{I_z - I_x}{I_y} \qquad J_z = \frac{I_x - I_y}{I_z} \tag{14a}$$

$$B = \tfrac{1}{2}\rho V^2 Sb \qquad C = \tfrac{1}{2}\rho V^2 S\bar{c} \tag{14b}$$

We can set the scaling constant to have the following form:

$$k = \sqrt{\frac{u_s^{\max}}{I_s}} \tag{15}$$

where $u_s^{\max}$ and I_s are scaling parameters that can be chosen arbitrarily (the values $u_s^{\max} = u_y^{\max}$ and $I_s = I_y$ were used in the study). Finally, we get

$$\dot{P} = J_x QR + J_{sx} a_x \delta_x + J_{sx} B_s C_l(\alpha,\beta,p,\Delta_a) \tag{16a}$$

$$\dot{Q} = J_y RP + J_{sy} a_y \delta_y + J_{sy} C_s C_m(\alpha,\beta,q,\delta_e) \tag{16b}$$

$$\dot{R} = J_z PQ + J_{sz} a_z \delta_z + J_{sz} B_s C_n(\alpha,\beta,r,\delta_r) \tag{16c}$$

where the constants introduced to abbreviate the notation are given by

$$J_{sx} = \frac{I_s}{I_x} \qquad J_{sy} = \frac{I_s}{I_y} \qquad J_{sz} = \frac{I_s}{I_z}$$

$$a_x = \frac{u_x^{\max}}{u_s^{\max}} \qquad a_y = \frac{u_y^{\max}}{u_s^{\max}} \qquad a_z = \frac{u_z^{\max}}{u_s^{\max}}$$

$$B_s = \frac{B}{u_s^{\max}} \qquad C_s = \frac{C}{u_s^{\max}} \tag{17}$$

The scaled mathematical model is used for defining the optimal control problems of interest and in the actual numerical computations of the extremal trajectories. The *state variables* are $(\alpha,\beta,\mu,P,Q,R)^T = \boldsymbol{x}$. As can be seen, μ is an ignorable state variable (i.e., it does not appear in the right-hand side of the state differential equations). However, when the translational motion of the aircraft is considered, μ is not ignorable.

III. Optimal Control Problem

Mathematical Model

The mathematical model of the aircraft is represented by the kinematical equations, Eqs. (12a–12c), and the dynamical equations, Eqs. (16a–16c), which are shown here in annotated form:

$$\dot{P} = \underbrace{\epsilon_t J_{sx} a_x \delta_x}_{L_t} + \underbrace{\epsilon_{\bar{q}} J_{sx} B_s C_l(\cdot)}_{L_a} + \underbrace{J_x QR}_{L_{qr}} \tag{18a}$$

$$\dot{Q} = \underbrace{\epsilon_t J_{sy} a_y \delta_y}_{M_t} + \underbrace{\epsilon_{\bar{q}} J_{sy} C_s C_m(\cdot)}_{M_a} + \underbrace{J_y RP}_{M_{rp}} \tag{18b}$$

$$\dot{R} = \underbrace{\epsilon_t J_{sz} a_z \delta_z}_{N_t} + \underbrace{\epsilon_{\bar{q}} J_{sz} B_s C_n(\cdot)}_{N_a} + \underbrace{J_z PQ}_{N_{pq}} \tag{18c}$$

where (abbreviating $\mathfrak{L} = \epsilon_{\bar{q}} J_{sx} B_s$, $\mathfrak{M} = \epsilon_{\bar{q}} J_{sy} B_s$, and $\mathfrak{N} = \epsilon_{\bar{q}} J_{sz} B_s$)

$$L_a = \mathfrak{L} C_l(\cdot) = \underbrace{\mathfrak{L} C_l^0(\alpha,\beta)}_{L_0} + \underbrace{\epsilon_\zeta \mathfrak{L} C_l^\zeta(\alpha,p)}_{L_\zeta} + \underbrace{\epsilon_c \mathfrak{L} A(\alpha)\Delta_a}_{L_c} \tag{19a}$$

$$M_a = \mathfrak{M} C_m(\cdot) = \underbrace{\mathfrak{M} C_m^0(\alpha,\beta)}_{M_0} + \underbrace{\epsilon_\zeta \mathfrak{M} C_m^\zeta(\alpha,q)}_{M_\zeta} + \underbrace{\epsilon_c \mathfrak{M} E(\alpha,\delta_e)}_{M_c} \tag{19b}$$

$$N_a = \mathfrak{N} C_n(\cdot) = \underbrace{\mathfrak{N} C_n^0(\alpha,\beta)}_{N_0} + \underbrace{\epsilon_\zeta \mathfrak{N} C_n^\zeta(\alpha,r)}_{N_\zeta} + \underbrace{\epsilon_c \mathfrak{N} R(\alpha)\delta_r}_{N_c} \tag{19c}$$

and

$$E(\alpha,\delta_e) = F(\alpha)\delta_e + G(\alpha) \tag{20}$$

It is assumed that C_l^c, C_m^c, and C_n^c, the components of the aerodynamic moment coefficients C_l, C_m, and C_n due to the primary aerodynamic control surfaces (ailerons, elevator, and rudders, respectively), depend linearly on the corresponding primary controls Δ_a, δ_e, and δ_r [also see Eq. (9)], through the functions $A(\alpha)$, $F(\alpha)$, $G(\alpha)$, and $R(\alpha)$. Since C_l^c, C_m^c, and C_n^c [Eq. (10)], besides the corresponding primary controls, depend on the angle of attack α only, one can easily imagine that a one-to-one map (transformation) can be established between the actual control surfaces deflections and the scaled primary controls Δ_a, δ_e, and δ_r, so that the latter appear linearly in C_l^c, C_m^c, and C_n^c, as before. Thus, for regular extremal trajectories, the extremal controls are bang-bang (see the following subsection on the optimality conditions). The formulation with linearly appearing controls was done for convenience in the numerical (algorithmic) minimization[11] of the variational Hamiltonian. For example, one can see that $A(\alpha) = \max\{C_l^c(\alpha,\Delta_a)\}$ for $\Delta_a \in [-1,+1]$. Similar relations hold for $F(\alpha)$, $G(\alpha)$, and $R(\alpha)$.

In the model, ϵ_t, $\epsilon_{\bar{q}}$, ϵ_ζ, and ϵ_c are *homotopy variables*; their role is explained later. However, it is noted that the mathematical model represents the physical system of interest when each homotopy variable has unit value. No state constraints are imposed.

Boundary Conditions and Cost Function

We want to guide the system from a given initial state to a given terminal state in minimum time. We consider a class of maneuvers that can be characterized by

$$\boldsymbol{x}_0 = \big[\alpha(t_0),\beta(t_0),\mu(t_0),P(t_0),Q(t_0),R(t_0)\big]^T = (\alpha_0,\beta_0,\mu_0,0,0,0)^T \tag{21a}$$

$$\boldsymbol{x}_f = \big[\alpha(t_f),\beta(t_f),\mu(t_f),P(t_f),Q(t_f),R(t_f)\big]^T = (\alpha_f,\beta_f,\mu_f,0,0,0)^T \tag{21b}$$

The cost function here is

$$J = \int_{t_0}^{t_f} f^0\big[\boldsymbol{x}(t),\boldsymbol{u}(t)\big]\,dt = \int_{t_0}^{t_f} 1\,dt = t_f - t_0 \tag{22}$$

Equations (21) and (22) define the class of minimum-time rest-to-rest reorientation maneuvers.

Adjoint Variables Dynamics

The dynamics of the adjoint variables $(\lambda_\alpha, \lambda_\beta, \lambda_\mu, \lambda_P, \lambda_Q, \lambda_R)^T = \boldsymbol{\lambda}$ are given by the following set of differential equations[8–10]:

$$\frac{d\lambda_v}{dt} = -\frac{\partial H}{\partial v}, \qquad v = \alpha,\beta,\mu,P,Q,R \tag{23}$$

where

$$H = H(\boldsymbol{\lambda},\boldsymbol{x},\boldsymbol{u}) = \lambda^0 f^0 + \sum_v \lambda_v \dot{v}(\boldsymbol{x},\boldsymbol{u}) \tag{24}$$

is the variational Hamiltonian of the system.

Optimality Conditions

Normality of the problem is assumed ($\lambda^0 = +1 > 0$). The variational Hamiltonian of the system is explicitly given by

$$\begin{aligned} H = {} & 1 + \lambda_\alpha\big[Q - (P\cos\alpha + R\sin\alpha)\tan\beta\big] \\ & + \lambda_\beta(P\sin\alpha - R\cos\alpha) + \lambda_\mu(P\cos\alpha + R\sin\alpha)\frac{1}{\cos\beta} \\ & + \lambda_P\big[\epsilon_t J_{sx} a_x \delta_x + \epsilon_{\bar{q}} J_{sx} B_s C_l(\alpha,\beta,p,\Delta_a) + J_x QR\big] \\ & + \lambda_Q\big[\epsilon_t J_{sy} a_y \delta_y + \epsilon_{\bar{q}} J_{sy} C_s C_m(\alpha,\beta,q,\delta_e) + J_y RP\big] \\ & + \lambda_R\big[\epsilon_t J_{sz} a_z \delta_z + \epsilon_{\bar{q}} J_{sz} B_s C_n(\alpha,\beta,r,\delta_r) + J_z PQ\big] \end{aligned} \tag{25}$$

Only the following part of the Hamiltonian depends on the control vector $u(t)=(\delta_x,\delta_y,\delta_z,\Delta_a,\delta_e,\delta_r)^T$:

$$H^c = +\lambda_P\left[\epsilon_t J_{sx} a_x \delta_x + \epsilon_{\bar{q}}\epsilon_c J_{sx} B_s A(\alpha)\Delta_a\right] + \lambda_Q\left[\epsilon_t J_{sy} a_y \delta_y + \epsilon_{\bar{q}}\epsilon_c J_{sy} C_s F(\alpha)\delta_e\right] + \lambda_R\left[\epsilon_t J_{sz} a_z \delta_z + \epsilon_{\bar{q}}\epsilon_c J_{sz} B_s R(\alpha)\delta_r\right] \quad (26)$$

As already mentioned, the thrust-vectoring controls δ_x, δ_y, and δ_z obey the following constraint:

$$|\delta_x|^n + |\delta_y|^n + |\delta_z|^n \le 1$$

For the case $n=2$, the extremal controls (which minimize the variational Hamiltonian) are computed from

$$\delta_x = -\frac{\lambda_P J_{sx} a_x}{\sqrt{(\lambda_P J_{sx} a_x)^2 + (\lambda_Q J_{sy} a_y)^2 + (\lambda_R J_{sz} a_z)^2}}$$

$$\delta_y = -\frac{\lambda_Q J_{sy} a_y}{\sqrt{(\lambda_P J_{sx} a_x)^2 + (\lambda_Q J_{sy} a_y)^2 + (\lambda_R J_{sz} a_z)^2}} \quad (27)$$

$$\delta_z = -\frac{\lambda_R J_{sz} a_z}{\sqrt{(\lambda_P J_{sx} a_x)^2 + (\lambda_Q J_{sy} a_y)^2 + (\lambda_R J_{sz} a_z)^2}}$$

The aerodynamic controls appear linearly in the system dynamics and are independent: Δ_a, δ_e, $\delta_r \in [-1,1]$. Therefore, the control domain $(\Delta_a,\delta_e,\delta_r)$ is a cube. When λ_P, λ_Q, and λ_R are not equal to zero, the optimality condition yields

$$\Delta_a = -\operatorname{sgn}\left[\lambda_P J_{sx} B_s A(\alpha)\right]$$

$$\delta_e = -\operatorname{sgn}\left[\lambda_Q J_{sy} C_s F(\alpha)\right] \quad (28)$$

$$\delta_r = -\operatorname{sgn}\left[\lambda_R J_{sz} B_s R(\alpha)\right]$$

The points where the adjoint variables λ_P, λ_Q, or λ_R cross (transversally) through zero are called *switching points*. At these points the corresponding control Δ_a, δ_e, or δ_r switches from $+1$ to -1 or vice versa and can conventionally be assumed zero. There might exist trajectories such that some of λ_P, λ_Q, or λ_R stay zero along a time interval of finite length. The existence of such trajectories (*singular trajectories*) has not been examined in the study.

Interpretation of the Results

A trajectory that satisfies the necessary conditions for optimality and the given boundary conditions is called an *extremal trajectory* or, briefly, an *extremal*. The sequence of switching points for a given extremal (i.e., their number and order) will be further referred to as the *switching structure* of the extremal.

Assuming that an optimal solution exists, the extremal that yields a minimum value of the cost function is the actual optimal trajectory. There is no easy test that can assure existence of a minimizer; moreover, the number of extremal solutions is unknown. In general, one should attempt to find all extremals. The computed extremal that renders minimum value to the cost function can be considered to be the *best* extremal. Engineering judgment and analyses can further help understand the nature of the extremals. One hopes eventually to explain the characteristics that make one of them better than any other found for a given reorientation maneuver.

Numerical Multipoint Boundary-Value Problem

By introducing a new unknown, the total time $T=t_f-t_0$, and appropriate number of switching points, the set of necessary conditions for optimality is cast into a numerical multipoint boundary-value problem.[15] A special software package,[16] designed for solving multipoint boundary-value problems with switching points and jumping conditions, was used.

Homotopy Approach

The resulting numerical multipoint boundary-value problems are extremely difficult to solve. They require a very good estimate of the unknowns [$\lambda(0)$, T, and the location of the switching points]. A homotopy approach was adopted throughout the study so that solutions to simpler problems were utilized to obtain solutions to more complex problems. First a number of extremals were found for two reorientation maneuvers in vacuum (90-deg bank and roll-around-the-velocity-vector maneuvers[11,17]). These correspond to a model with the dynamic pressure homotopy parameter $\epsilon_{\bar{q}}=0$. Further, extremals were obtained by gradually increasing $\epsilon_{\bar{q}}$ from 0 to 1, with full damping ($\epsilon_\zeta=1$) and no aerodynamic control power ($\epsilon_c=0$). Next, the aerodynamic control surface contribution was accounted for by increasing ϵ_c from 0 to 1. This was done in a few steps, since a fairly good estimate of the location and the structure of the switching points is needed for the numerical methods used in solving the MPBVPs. Further details about this procedure can be found in Ref. 11. Finally, the thrust-vectoring homotopy parameter ϵ_t was gradually decreased from 1 to 0 and results for an aircraft without thrust-vectoring obtained.

The essence of the homotopy method is that a solution to a particular problem can serve as a good initial guess for a new MPBVP, which differs from the previous one by a small perturbation in the model parameters or the boundary conditions. Thus, starting from a known extremal, by varying a model parameter (or the boundary conditions) one can get a series of extremals, solutions to a number of MPBVPs. Such a series of extremals will be referred to as a *family of extremals.*

IV. Numerical Results

Results about extremal solutions for two types of reorientation maneuvers are presented. The first type of maneuver (maneuver 1) is customarily called a roll-around-the-velocity-vector maneuver and is characterized by the following initial and final states: $x_0=(\alpha_0,0,0,0,0,0)^T$ and $x_f=(\alpha_f,0,\mu_f,0,0,0)^T$, with $\alpha_0=\alpha_f$. Only the case $\mu_f=90$ deg is considered. A maneuver of this type can be specified by a single constant $\alpha_{0f}(=\alpha_0=\alpha_f)$.

The second type of maneuver (maneuver 2) is characterized by the following initial and final states: $x_0=(10^0,0,0,0,0,0)^T$ and $x_f=(\alpha_f,0,90^0,0,0,0)^T$. This maneuver can be specified by a single constant α_f. This maneuver can be viewed as reorientation of an aircraft from an initial steady-state, straight, and level flight to a certain direction in the horizontal plane, with no sideslip angle.

These two maneuvers are of interest for themselves but also may be considered to be part of a more complex, composite maneuver in a combat situation. Imagine the aircraft performing maneuver 2 first, firing a missile, then changing its attitude by performing maneuver 1, and firing another missile in the corresponding direction. By varying the angles α_{0f} or α_f and the initial and final orientation (or the final orientation only) of the aircraft, we can get a series of extremal trajectories, all belonging to one family of extremal solutions.

Description of an Extremal

Details about one particular extremal trajectory are presented in Figs. 1a–1l. The extremal corresponds to maneuver 1 for $\alpha_{0f}=30$ deg. It is possible to perform this maneuver so that α is kept practically constant and the sideslip angle close to zero. For smaller values of α, this can be done by yawing (e.g., full rudders) while rolling and adjusting the elevator as necessary to keep α constant and β zero. An extremal was found that resembles this motion. Some numerical studies suggest that such a regular extremal exists if the aircraft does not possess "too much" roll power. However, the aircraft considered possesses a lot of roll power, especially at lower angles of attack (from the ailerons). The extremal we present is quite different in nature.

As can be seen from Figs. 1a and 1c, the aircraft pitches down during the first part of the trajectory, then pitches up during the rest of the maneuver. The aircraft rolls and yaws in the positive direction all of the time, as one would expect. Figure 1b shows the orientation of the aircraft in time in terms of the standard set of Euler angles (one can visualize the attitude of the aircraft easier in these terms). The adjoint variables λ_P, λ_Q, and λ_R, which are responsible for the determination of the extremal controls, are shown in Fig. 1d. The aerodynamic and the thrust-vectoring controls are shown in Figs. 1e and 1f. The essential feature of this maneuver is that the aircraft pitches down and up because it has a lot of pitch power from the elevator and from the thrust-vectoring system and because at lower α the ailerons are more powerful. The relative magnitude (proportion) of power the aircraft has for roll, pitch, and yaw can be seen from Figs. 1g, 1i, and 1k. The individual contribution of the thrust-vectoring system, the aerodynamic moments, and the gyroscopic moments [Eqs. (18a–18c)] can be seen, too. A remarkable feature of this extremal is that most of the time throughout the maneuver the gyroscopic moments tend to support the thrust-vectoring and aerodynamic control surface generated moments. The gyroscopic

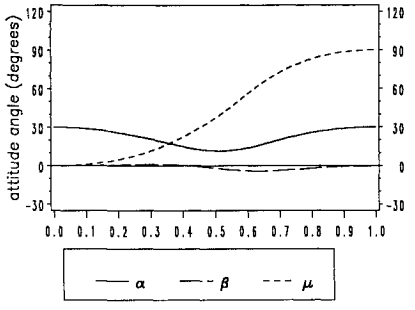

Fig. 1a Angles α, β, and μ vs scaled time.

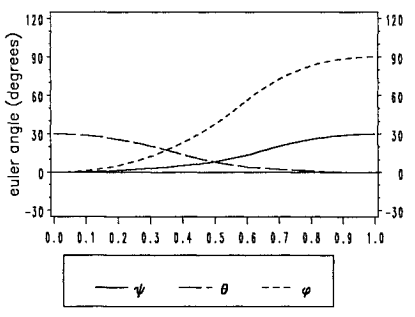

Fig. 1b Euler angles ψ, θ, and φ vs scaled time.

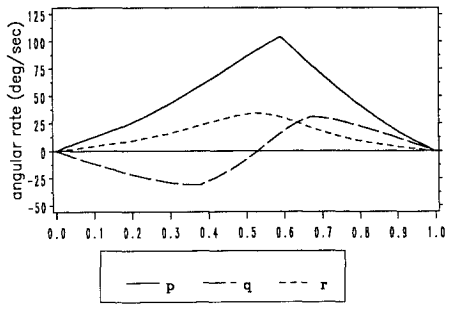

Fig. 1c Angular rates (roll, pitch, and yaw) vs scaled time.

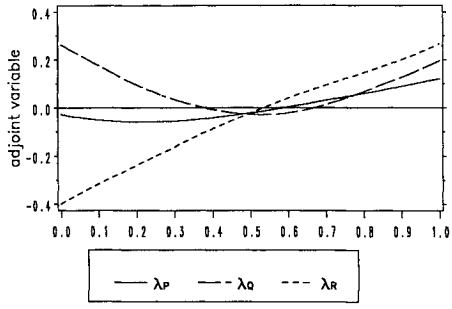

Fig. 1d Angular-rate adjoint variables vs scaled time.

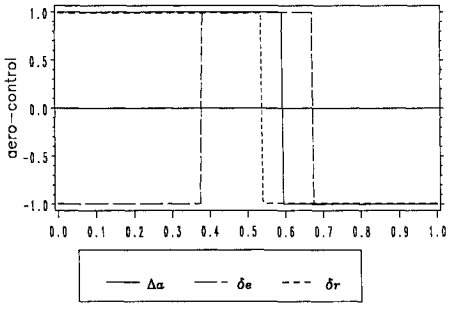

Fig. 1e Aerodynamic controls vs scaled time.

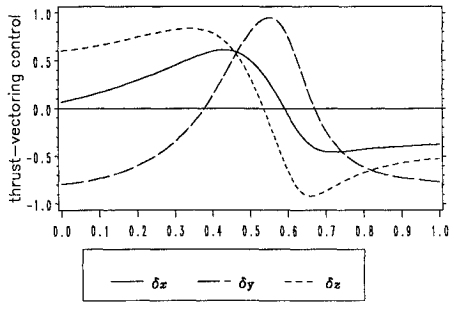

Fig. 1f Thrust-vectoring controls vs scaled time.

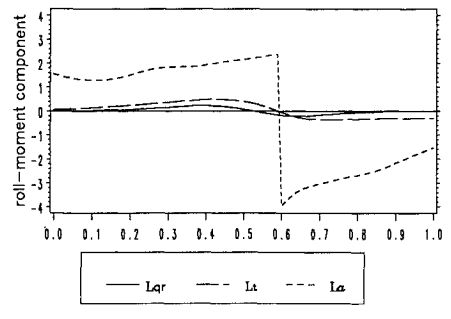

Fig. 1g Roll dynamics components vs scaled time.

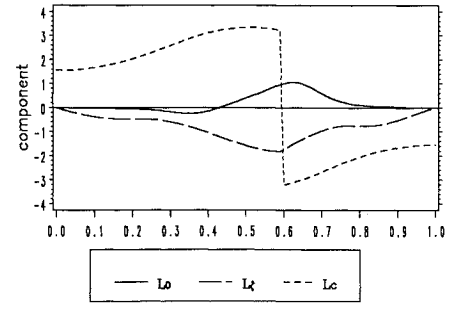

Fig. 1h Aerodynamic roll components vs scaled time.

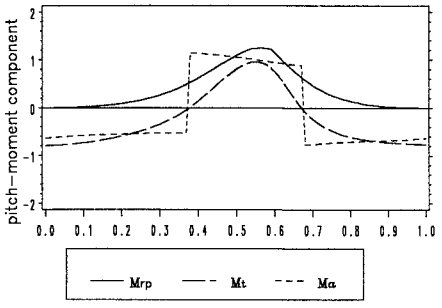

Fig. 1i Pitch dynamics components vs scaled time.

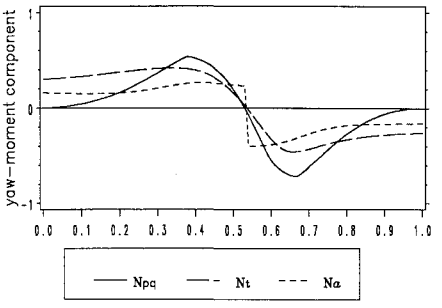

Fig. 1k Yaw dynamics components vs scaled time.

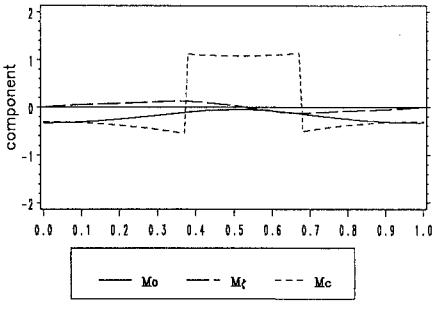

Fig. 1j Aerodynamic pitch components vs scaled time.

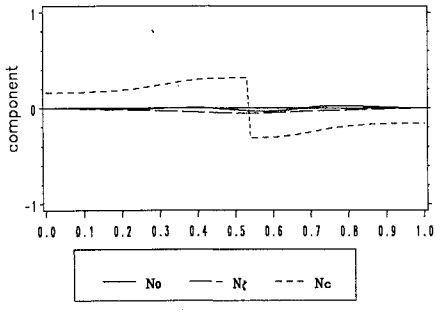

Fig. 1l Aerodynamic yaw components vs scaled time.

term in the yaw channel is more powerful than the control power and acts quite supportively (Fig. 1k). The same is true for the pitch channel (Fig. 1i).

The individual contributions of the aerodynamic terms can be seen in Figs. 1h, 1j, and 1l [see also Eqs. (19a–19c)]. The maneuver does not take a lot of advantage of the dihedral effect: the sideslip angle tends to stay below 5 deg, which is a desirable feature since higher β means higher side accelerations that are not acceptable for the human pilot. The dihedral effect seems to have a supportive role in the (normalized) time interval from 0.4 to 0.6 only (see Fig. 1h). As a remark, we note here that, when analyzing extremal problems of the type considered, one must always keep in mind that there might be some tradeoffs on local level (in time) that better the extremal globally.

The extremal described is the only one found for the selected nominal value of the aircraft parameters. As mentioned, another extremal family is found for an aircraft possessing less roll power. Since the minimum principle requires the controls to be used in a certain way (to minimize the variational Hamiltonian), it is understandable why, given the initial and final state, an extremal family might cease to exist as the aircraft design parameters are varied. The domain of existence of a regular extremal depends on the relative amount of control power the aircraft possesses for roll, pitch, and yaw. It appears that the aircraft control power is well balanced for the maneuver and particular extremal trajectory considered.

Comparison of Results

Two subfamilies of extremals are shown in Fig. 2a. They show the maneuvering time of the aircraft for maneuver 1 type of reorientation problems. The lower line corresponds to the aircraft with the set of nominal design parameters, whereas the upper line corresponds to an aircraft without thrust-vector control ($\epsilon_t = 0$). The solid dots merely show some of the members of the family of extremals that have been evaluated by varying the initial and final value of α. The circles show the points where the switching structure changes. The switching structure shown in Fig. 1e is the simplest one. In the other switching structures, some of the switching points swap (change their order) and/or new switching points emerge (at the beginning or at the end of the trajectory). The dotted line represents a region where the switching structure changes very rapidly (about half a dozen different switching structures on an interval of less than 5 deg). This rapid change of the switching structures in those regions indicates higher sensitivity of the solution. From Fig. 2a one can easily estimate the gain in maneuvering time, due to the thrust-vectoring enhancement, for the reorientation maneuvers considered.

In Fig. 2b the maneuvering time is shown for two subfamilies of extremals for maneuver 2 type of reorientation problems (all of the extremals discussed in this paper indeed belong to one single family and can be numerically derived from each other by gradually varying the maneuver boundary conditions and/or the model parameters). As before, the lower line corresponds to an aircraft with thrust-vectoring capability and the upper one to an aircraft without thrust-vectoring capability. Below 35 deg, the family ceases to exist for an aircraft without thrust-vectoring capability. Although we have not thoroughly examined this feature, it appears that the aircraft has unproperly balanced roll, pitch, and yaw power for these reorientation maneuvers.[18] The evolution of the adjoint variables suggests that singular extremals might emerge and exist for maneuvers with smaller α_f.

Amount of Thrust-Vectoring Power

Figure 3a shows results for two subfamilies of extremals obtained by varying the homotopy parameter ϵ_t above and below its nominal value. One can give a physical interpretation of the mathematical model as corresponding to an aircraft with a more or less powerful thrust-vectoring system (e.g., by varying the size of the paddles that deflect the jetstream). The results correspond to $\alpha_{0f} = 30$ and 50 deg. The asterisks denote the maneuvering time for the nominal value of thrust-vectoring power (observe Fig. 2a, lower line). As can be seen, by decreasing the thrust-vectoring power, maneuvering time increases significantly. However, by increasing the thrust-vectoring power, maneuvering time improves negligibly. One can conclude that, for the two classes of reorientation maneuvers and for the family of extremal motions considered, the nomi-

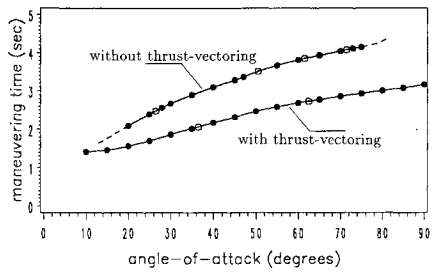

Fig. 2a Maneuver 1: maneuvering time vs α_{0f}.

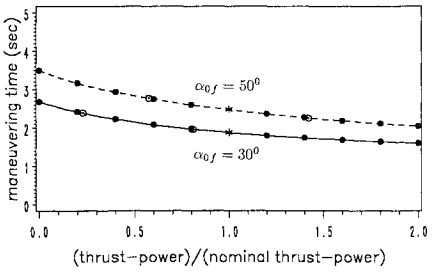

Fig. 3a Maneuver 1: maneuvering time vs TV power.

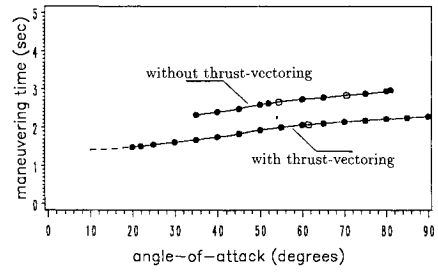

Fig. 2b Maneuver 2: maneuvering time vs α_f.

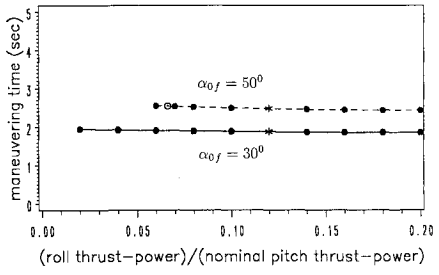

Fig. 3b Maneuver 2: maneuvering time vs TV roll power.

nal value of the thrust-vectoring power is a good choice. By examining similar plots for a variety of reorientation maneuvers and extremals, one can make a good engineering decision (usually associated with other engineering tradeoffs) about an actual implementation of a thrust-vectoring system.

In Fig. 3b the thrust-vectoring roll power is varied, while keeping the pitch and yaw power at their nominal value, and subfamilies of extremals are obtained for the same maneuvers as those in Fig. 3a. This is done by varying the a_x parameter in the mathematical model [Eqs. (18a–18c)]. The nominal value of a_x is 0.12. Below certain values of a_x the families could not be extended. The evolution of the adjoint variables λ_P, λ_Q, and λ_R suggests that singular extremals may emerge as a_x is decreased further. As can be seen, for these maneuvers and the extremal considered, maneuvering time does not change significantly as the thrust vectoring roll power varies over a broad range of values. This is due to the already described peculiar nature of the extremal. The aircraft pitches down to lower α since there the ailerons have a lot of roll power, which is much greater than the thrust-vectoring system can produce. By examining similar plots, for a variety of maneuvers and extremals, a designer might make a decision about how much thrust-vectoring roll power the aircraft should possess. The designer must also include in the analysis the fact that thrust-vectoring roll power is needed at high α (where the ailerons are not effective). In actual flight, the aircraft is subjected to disturbances. If a control system is implemented for automatic guidance of the aircraft in the course of the reorientation maneuvers, it should be composed of an open-loop controller and a closed-loop control subsystem (which will cope with the disturbances and the measurement error). For post-stall flight the closed-loop control system will certainly require thrust-vectoring roll power. Another criterion for the designer might be a desire for fault tolerance: in the case of mechanical failure of the ailerons, the thrust-vectoring roll power can be used to safely land the aircraft.

V. Conclusions

By accurately modeling the aircraft dynamics (in particular, the aerodynamic and propulsive moments), it was possible to investigate numerically certain problems of time-optimal fuselage reorientation of the high angle-of-attack research vehicle. The control power of the thrust-vectoring system was parameterized so that its effect on system performance could be studied. The results for two classes of reorientation maneuvers suggest that it is worth enhancing the aircraft with thrust-vectoring capability. The savings in maneuvering time are about 20–30%. More detailed studies, coupled with studies of the basic aerodynamic properties of the aircraft, can lead to useful design rules. This work shows that it is possible to use optimal control theory, in conjunction with sensible interactive engineering techniques, to analyze and solve optimal-control problems for highly complex dynamical systems.

Acknowledgments

This work was supported in part by the Air Force Office of Scientific Research under Grants AFOSR-89-0001 and AFOSR-92-J-0078, and in part by NASA Langley Research Center under Grant NAG-1-1405. Data for the HARV were supplied by Chris Gracey, Carey Buttrill, and Aaron Ostroff from the Aircraft Guidance and Control Branch, and Keith Hoffler from the Flight Dynamics Branch, NASA Langley Research Center.

References

[1]Herbst, W. B., "Future Fighter Technologies," *Journal of Aircraft,* Vol. 17, No. 8, 1980, pp. 561–566.

[2]Herbst, W. B., "Dynamics of Air Combat," *Journal of Aircraft,* Vol. 20, No. 7, 1983, pp. 594–598.

[3]Well, K. H., Farber, B., and Berger, E., "Optimization of Tactical Aircraft Maneuvers Utilizing High Angles of Attack," *Journal of Guidance, Control, and Dynamics,* Vol. 5, No. 2, 1982, pp. 131–137.

[4]Ashley, H., "On the Feasibility of Low-Speed Aircraft Maneuvers Involving Extreme Angles-of-Attack," *Journal of Fluids and Structures,* Vol. 1, July 1987, pp. 319–335.

[5]Lacey, D. W., "Air Combat Advantages from Reaction Control Systems," Society of Automotive Engineers Aerospace Congress and Exposition, TP 801177, Los Angeles, CA, Oct. 13–16, 1980.

[6]Gal-Or, B., *Vectored Propulsion, Supermaneuverability and Robot Aircraft,* Springer-Verlag, New York, 1989.

[7]Bundick, T., private correspondence, AGCB NASA Langley Research Center, June 1990.

[8]Bryson, A. E., Jr., and Ho, Y. C., *Applied Optimal Control,* Hemisphere, New York, 1975.

[9]Pontriagin, L. S., Boltyanskii, V. G., Gamkrelidze, R. V., and

Mishchenko, E. F., *The Mathematical Theory of Optimal Processes,* Interscience, New York, 1962.

[10]Alekseev, V. M., Tikhomirov, V. M., and Fomin, S. V., *Optimal Control,* Consultants Bureau, New York and London, 1987.

[11]Bocvarov, S., "Time-Optimal Reorientation Maneuvers of an Aircraft," Ph.D. Dissertation, Aerospace and Ocean Engineering Dept., Virginia Polytechnic Inst. and State Univ., Blacksburg, VA, Aug. 1991.

[12]Junkins, J. L., and Turner, J. D., *Optimal Spacecraft Rotational Maneuvers,* Elsevier, New York, 1986.

[13]Goldstein, H., *Classical Mechanics,* 2nd ed., Addison-Wesley, Reading, MA, 1980.

[14]Etkin, B., *Dynamics of Atmospheric Flight,* Wiley, New York, 1972, pp. 104–128.

[15]Stoer, J., and Bulirsch, R., *Introduction to Numerical Analysis,* Springer-Verlag, New York, 1980.

[16]Oberle, H. J., and Grimm, "BOUNDSCO—A Program for Numerical Solution of Optimal Control Problems," English translation of DFVLR-Mitt. 85-05, ICAM—Virginia Polytechnic Inst. and State Univ., Blacksburg, VA, May 1989.

[17]Chowdhry, R. S., and Cliff, E. M., "Optimal Rigid-Body Motions," *Journal of Guidance, Control, and Dynamics,* Vol. 2, No. 2, 1991, pp. 383–390.

[18]Bocvarov, S., Cliff, E. M., and Lutze, F. H., "The Balance and Harmony of Control Power for Combat Aircraft in Tactical Maneuvering," AIAA Paper 92-4636, Aug. 1992.